Journal of Polymers and the Environment (2022) 30:4178–4192
https://doi.org/10.1007/s10924-022-02497-z

ORIGINAL PAPER

Synthesis, Characterization, and Potential Evaluation of Modified Cellulose Immobilized with Hydroxyquinoline as a Sorbent for Vanadium Ions

Amal E. Mubark[1] · Ahmed A. Eliwa[1] · Salah A. Zaki[1] · Basma T. Mohamed[1]

Accepted: 30 May 2022 / Published online: 25 June 2022

Abstract
A considerable increase in the importance of vanadium globally and its common uses in many manufacturable alloys made it a target for much scientific research interested in extraction and recovery. A solid modified cellulose sorbent (GCIHQ) was prepared by simple grafting of cellulose, then immobilized with hydroxyquinoline, and examined as a sorbent for V(V) ions. FT-IR, TGA, BET, and SEM–EDX investigations were used to characterize the GCIHQ. A higher surface area for the synthesized GCIHQ resin has been recorded (65.8 m^2/g) more than the used cellulose (21.7m^2/g). Several vanadium sorption parameters using the modified GCIHQ from the sulfate medium were optimized namely contact time, pH, initial vanadium ions concentration, sorbent dose, and sorption temperature. The kinetics results revealed that the sorption of vanadium ions upon the synthesized sorbent followed the pseudo-second-order with R^2 of > 0.99, which indicated that the sorption mechanism was chemical interaction. The sorption process was studied using Freundlich, Langmuir, Dubinin–Radushkevich, and Temkin isotherm models to describe the adsorbent-adsorbate interaction. The Langmuir model was the most fitting model with the experimental results; the experimental adsorption uptake of 113 mg/g was matched with that of the calculated results. The activation energy (E_a) for adsorption was 12.91 kJ.mol^{-1}, indicating the process is to be chemisorption. Thermodynamic characteristics with ΔH of 13.46 kJ/mol and a ΔS 115.15 J/mol.K revealed the endothermic and spontaneous nature.

Keywords Sorption · Cellulose · V(V) ions · Hydroxyquinoline · D-R and Temkin isotherms · Thermodynamics

Introduction

Vanadium is the fifth most common transition metal on the earth [1]. When it is highly pure, it is a soft, silvery, gleaming metal with ductile qualities [2]. One stable isotope V^{51} and one radioactive isotope V^{50} make up naturally occurring vanadium. The latter has a natural abundance of 0.25%and a half-life of 1.5×10^{17} years, whereas V^{51} has a natural abundance of 99.75%. It has oxidation states ranging from + 1 to + 5, however, it is most typically found in the + 4 as tetravalent vanadyl (VO_2^+) and in the + 5 states as pentavalent vanadate (HVO_4^{2-}, VO_3^- and/or $H_2VO_4^-$) species in natural and biological systems [3, 4]. Vanadium may be found in 65 various minerals, including carnotite, vanadinite, and patronite that regarded as an important source of vanadium [5].

Almost 85% of vanadium consumption is used in ferrovanadium production or as a steel additive [1] to improve the steel strength significantly [6]. Many important constituents were made of vanadium steel as gears and bicycle frames. Because vanadium alloys have poor neutron absorption properties and do not deform in creeping at high temperatures, they are employed in nuclear reactors [7]. Jet engines, airframes, and dental implants all use titanium-vanadium alloys [8]. Superconductive magnets are made from vanadium-gallium alloys. The use of lithium vanadium oxide as a high energy density anode for lithium-ion batteries has been proposed [9]. In the secondary aluminum industry, a grain refiner made of titanium-boron-aluminum (TiBAl) rod with less than 1% vanadium is employed.

The pollution gets from the vanadium element are predicted to rise as a result of fast developments for some industries. If vanadium sediments are exposed to acidic circumstances (pH ≤ 2), pollution of water bodies and soil is a

✉ Amal E. Mubark
amal_mubark2014@yahoo.com

[1] Nuclear Materials Authority, 530 Maadi, Cairo 11835, Egypt

distinct possibility [10]. The removal of vanadium pollution from wastewaters, groundwater, and soils is important for the environment, in addition to the economic value of the vanadium retrieval operations [11, 12].

Adsorption has recently emerged as one of the cheapest selective strategies [13–15] for separating vanadium. Trials were reported to have been conducted in order to establish an efficient procedure for extracting vanadium from their ores [12–16, 16–20]. In general, the development of "greener" and more environmentally friendly treatment technologies must be viewed as a critical component for enterprises dealing with toxic, hazardous, and chemically-laden wastewater [21–26]. Biopolymers have attracted a lot of attention because of their environmentally beneficial, non-toxic, and biodegradable properties. Because of their exceptional structural and physical properties, as well as their safety, availability, and economics, they are a very promising choice for the development of sustainable materials. Alginate, chitin, chitosan, cellulose, pectin, starch, and guar gum are organic biopolymers made up of the repeating unit of monosaccharaides [$C_n(H_2O)_n$] having both sustainable and environmentally beneficial [27]. Cellulose is one of the most well-known biopolymers because of its chemical, mechanical, and hydrophilicity capabilities, as well as its durability [28].

The purpose of this paper was the production of grafted cellulose immobilized with hydroxyquinoline (GCIHQ) and investigation its ability to retrieve V(V) ions from synthetic and effluent samples to be used in further industrial applications. Physical and chemical approaches were used to characterize the GCIHQ sorbent. Using the batch technique, various parameters impacting the adsorption process of V(V) ions on GCIHQ were examined. Thermodynamics, kinetics, and isotherm modeling for vanadium adsorption processes were explored and discussed. A real case study was conducted, as well as studies on the regeneration of modified cellulose sorbents.

Experimental

Reagents and Apparatus

Glycidyl-methacrylate GMA ($C_7H_{10}O_3$, assaying 97%), N,N'-methylene-bis-acrylamide MBA ($C_7H_{10}N_2O_2$, 99%), benzoyl peroxide (Bz_2O_2) ($C_{14}H_{10}O_4$, 75%), N,N-Dimethylformamide DMF ($C_3H_7N_O$, 98%), and 8-Hydroxyquinoline (C_9H_7NO, 98%) have been purchased from Sigma-Aldrich. All other chemicals, alcohols, and solvents were purchased from Prolabo-chemicals and used as received. Double distilled water (DDW) was used in all experiments. On the other hand, a stock solution of 1000 mg/L V(V) ions was prepared by dissolving 1.7851 g of di-vanadium-pentoxide (V_2O_5, 99.6%, Sigma-Aldrich) in 20 mL concentrated H_2SO_4 then diluted to 1 L using DDW. The concentrations of V(V) ions were estimated spectrophotometrically using dodeca-tungstophosphoric acid [29]. Metal ions in the non-synthetic sample were checked using inductively induced plasma (ICP), whereas sulfate and chloride anions were quantified using the titration method.

A Pye-Unicam Sp-883 spectrophotometer was used for Fourier transform infrared (FT-IR) spectra measurements between 4000 and 400 cm^{-1} using the KBr technique (ground finely sample pelletized in KBr, 1% w/w). By a Shimadzu DT/TG-50 instrument, thermogravimetric analysis (TGA) was performed using a heating rate of 10°/min in a nitrogen atmosphere. The nitrogen flow rate was set at 20 ml per minute. Using a Quanta chrome NOVA automated gas sorption system and N_2 gas as the adsorbate, the surface area and pore distribution were computed at 77 ± 1 K using the Brunauer–Emmett–Teller (BET) and Barrett–Joyner–Halenda (BJH) equations. An environmental scanning electron microscope was used to analyze the morphology of the adsorbent particles (SEM). The energy-dispersive X-ray (EDX) system (CAM SCAN series 4 ISIS 200 E/X system) with pentajet detector was used to detect components on the surface of adsorbents. Metal ions in the real sample were checked using ICP (720 ICP-OES, Agilent Technologies), whereas sulfate and chloride anions were quantified using the titration method. Using an Adwic pH meter, the concentration of hydrogen ions in the various solutions was determined.

Grafted Cellulose Formulation (CG)

10 g of cellulose were dispersed in 100 mL distilled water in a flask. The liquid was then spiked with 19 mL GMA and 1 g MBA. 0.12 g (Bz_2O_2) (initiator) was also added to the mixture while stirring. Also added to the cellulose-GMA mixture was a combination of one mL isopropyl alcohol and 25 mL cyclohexane. All of the ingredients were combined in a flask containing 145 mL (%) polyvinyl alcohol dissolved in isopropanol and heated for 3 h in a water bath at 70–80 °C with constant stirring [30]. Grafted cellulose (GC) is a thick white precipitate that was generated, filtered out, rinsed with ethanol and distilled water, and then dried in the air.

Immobilization of GC with 8-Hydroxyquinoline

2 g of 8-hydroxyquinoline were dissolved in 24 mL DMF, then 2 g of GC was spread on top of the solution. The mixture was heated to 90 °C in an oil bath for 72 h with constant stirring [31]. The precipitate was filtered out and washed with cold methanol and distilled water until it achieved a pH of 7.0. After drying for 24 h at room temperature, the product was given the name GCIHQ.

Chemical Stability Studies of GCIHQ

The chemical stability of the synthesized sorbent for acidic and alkaline media was tested by soaking a definite weight from the synthetized GCIHQ sorbent in 100 mL of 0.5 M from H_2SO_4 and NaOH each separately. By soaking the GCIHQ in the acid and alkaline medium for 24 h, the stability of the sorbent was measured by comparing the filtered off, washed with distilled water, and dried with the untreated synthetized GCIHQ sorbent.

Batch Experiments

The effects of various experimental conditions on the adsorption of vanadium ions were investigated. Solution pH, contact time, sorbent dose, and starting vanadium ion concentrations were among the parameters studied. Diluted HCl and NaOH were used for adjusting the pH of the aqueous medium. The batch technique was used to conduct the adsorption tests by agitating a definite weight from GCIHQ sorbent in a specific solution volume that has a definite vanadium concentration in an appropriate glass flask. These studies were carried out on a hotplate magnetic stirrer at room temperature for 2 h at a fixed stirring speed of 300 rpm. After equilibration, GCIHQ was filtered and the retained metal ion concentration (C_f) was measured spectrophotometrically. Adsorption parameters, variable ranges, and fixed conditions for each parameter were illustrated and abbreviated in Table 1. The mass balance equation was used to calculate the sorption capacity (q_e) (Eq. 1):

$$q_e = \left(C_i - C_f\right) \times V/m \tag{1}$$

q_e: the uptake (mg/g), C_i: the starting concentrations, C_f: the final concentrations of the metal ion under study (mg/L), m: the weight of the prepared resin (g), V: the volume (L).

All of the experiments were repeated three times, and the standard deviation was used to obtain the averaged results. The effects of co-existing ions were studied by mixing the same concentration from the co-existing studied ions (Y, Cr, Fe, U, Nb, Ce, Zr, and Ti) with an initial vanadium concentration of 200 mg/L. The adsorption efficiency of V(V) ions was tested using the previously optimized sorption conditions namely; 0.01 g resin 10 ml Aq., 200 mg/L V(V) ions, 200 mg/L Co-existing ion, pH 4, and agitating for 1 h at 25 °C.

Adsorption Isotherms, Kinetics, and Thermodynamics

Portions from the GCIHQ sorbent weighing 10 mg were inserted in flasks containing 10 mL of solutions containing V(V) ions at pH 4. The mixtures were for times ranging from 15 to 120 min and at temperatures ranging from 25 to 55 °C. A definite volume from the raffinate solution of the previous experiments was collected at the end of each one, and the adsorption uptake was estimated using Eq. 1. The adsorption results were used for computing the kinetics and thermodynamics of the vanadium adsorption processes on the GCIHQ sorbent. Adsorption isotherms were determined using the starting metal ions concentration test results.

Three equations were tested to determine the kinetics of V(V) ions adsorption on GCIHQ sorbent using the agitation time experimental results. The pseudo-first-order (PFO), pseudo-second-order (PSO) and intraparticle diffusion models were utilized to analyze the resulted date of the adsorption processes. The three models were represented as following in Eqs. (2–4) [32–34].

$$\log\left(q_e - q_t\right) = \log q_e - \left(\frac{k_1}{2.303}\right)t \tag{2}$$

$$\frac{t}{q_t} = \frac{1}{k_2 q_e^2} + \frac{1}{q_e}t \tag{3}$$

$$q_t = K_i t^{0.5} + X \tag{4}$$

q_e: the equilibrium adsorption capacity, q_t: the adsorption capacity at time t, k_1, k_2, and K_i: the reaction rate constants for the PFO, PSO, and intraparticle diffusion models. X: constant and proportional to the thickness of the boundary layer.

The adsorption mechanism was determined and explained based on studying various isotherms namely; Langmuir, Freundlich, Dubinin–Radushkevich (D-R), and Temkin empirical models which represented as following in Eqs. (5–7 and 10) [35–38].

Table 1 the adsorption parameters of V(V) ions using the synthesized GCIHQ sorbent

Adsorption factors	Variable range	Fixed conditions
pH	1–5	0.01 g resin, 10 ml Aqueous, 200 mg/L V ions, 25 °C, 1 h
Stirring time, min	15–120	0.01 g resin, 10 ml Aqueous, 200 mg/L V ions, 25 °C, pH = 4
Initial V ions conc., mg/L	100–500	0.01 g resin, 10 ml Aqueous, 25 °C, pH = 4, 1 h
Sorbent dose, g	0.01–0.05	10 ml Aqueous, 200 mg/L V ions, 25 °C, pH = 4, 1 h
Stirring temp., °C	25–55	0.01 g resin, 10 ml Aqueous, 200 mg/L V ions, pH = 4, 1 h

$$\frac{C_e}{q_e} = \frac{C_e}{q_{max}} + \frac{1}{q_{max} K_L} \quad (5)$$

$$\log(q_e) = \log K_f + \frac{1}{n}\log C_e \quad (6)$$

$$\ln q_e = \ln q_m - \beta\varepsilon^2 \quad (7)$$

$$\varepsilon = RT\ln(1 + \frac{1}{C_e}) \quad (8)$$

$$E = 1/\sqrt{2B} \quad (9)$$

$$q_e = \left(\frac{RT}{b_T}\right)\ln A_T + \left(\frac{RT}{b_T}\right)\ln C_e \quad (10)$$

q_e: the equilibrium adsorption capacity, q_m: the maximum adsorption capacity, k_L: the Langmuir constant related to the adsorption capacity, C_e: the vanadium concentration in solution.

k_F and 1/n: the Freundlich constant related to adsorption capacity and intensity, respectively. K_{DR}: the maximum adsorption capacity in mol/g, B: the constant related to the adsorption energy in mol /kJ, E (KJ/mol), Ɛ: the Polanyi potential.

(RT/b_T): constant in relation to the heat of adsorption, A_T: the binding constant at equilibrium related to the maximum binding energy, R: the gas constant (8.314 kJ/mol K), T: the temperature (K).

Desorption and Regeneration Experiments

Desorption of V(V) ions from the loaded sorbent was realized through contact of the loaded GCIHQ with a definite volume of various eluents and agitated together for 30 min with 300 rpm at room temperature. After choosing the optimal desorption conditions, GCIHQ was filtered and rinsed with distilled water before being reused in additional adsorption rounds using the optimal adsorption and desorption parameters. The regeneration efficiency (%) was calculated according to Eq. 11.

$$\text{Regeneration efficiency}\% = \frac{\text{uptake in}(n+1)^{th}\,\text{run} \times 100}{\text{uptake in}(n)^{th}\,\text{run}} \quad (11)$$

n was equal to 1 or 2 or 3, etc.

Application on Laboratory Effluent Solution

The recovery of vanadium content from waste solutions collected from production sector laboratories in the Egyptian Nuclear Materials Authority (NMA) was studied using the synthesized GCIHQ sorbent. A waste solution of 2.8 pH and containing 1910 mg/L V(V) ions with other metal gangues was analyzed as shown in Table 2. Conventional wet chemical analytical techniques and ICP-OES were used for analyzing the major oxides and the trace elements. The optimized adsorption conditions of V(V) ions from the waste solutions upon the studied sorbent were performed. The loaded resin was subjected to complete desorption for the loaded V(V) ions and the eluate solution was precipitated using ammonia solution at pH 7.5. The dried precipitate was instrumentally analyzed using EDX to identify the product constituents.

Results and Discussion

Chemical and Physical Characterization of the Prepared GCIHQ

The chemical modification of cellulose by 8-Hydroxyquinoline moieties was carried out through grafting polymerization of glycidyl-methacrylate and N,N'-methylene-bis-acrylamide on the cellulose support. The grafting process was carried out using (Bz_2O_2) as an initiator. The grafting copolymerization process was started by initiating free radical sites on the cellulose backbone which act as active centers. The reaction route is given in Scheme 1.

FT-IR Analysis

FT-IR spectra of cellulose, GC, and GCIHQ sorbent before and after adsorption were presented in Fig. 1a. Absorption bands at 3352, 2898, and 1161 cm^{-1} were detected in the cellulose spectra, and these bands were attributed to hydrogen-bonded –OH, C–H, and anti-symmetric stretching vibrations of the C–O–C bridge [39–42]. The additional new band at 1728 cm^{-1} (C = O), 906, and 850 cm^{-1} showed in the spectrum of GC assigned to the presence of the epoxide group [43]. Unfortunately, NH cannot be detected due to its overlapping with the broad OH band at 3413 cm^{-1}. The epoxide bands in GCIHQ's IR spectra nearly completely vanished at wavenumbers 849 and

Table 2 Chemical analysis of the effluent solution sample before and after adsorption

Constituent	V	Cu	Cd	REE	Th	Zr	Ti	Si	SO_4^{-2}	Cl-	Na	K
Before Ads. Conc., mg/L	1910	78	92	103	29	49	2500	580	24,000	1000	40,328	520
After Ads. Conc., mg/L	1766	75	92	101.5	28	48	2488	201	18,140	678	36,130	512

Scheme 1 Simplified representation for the synthetized GCIHQ sorbent

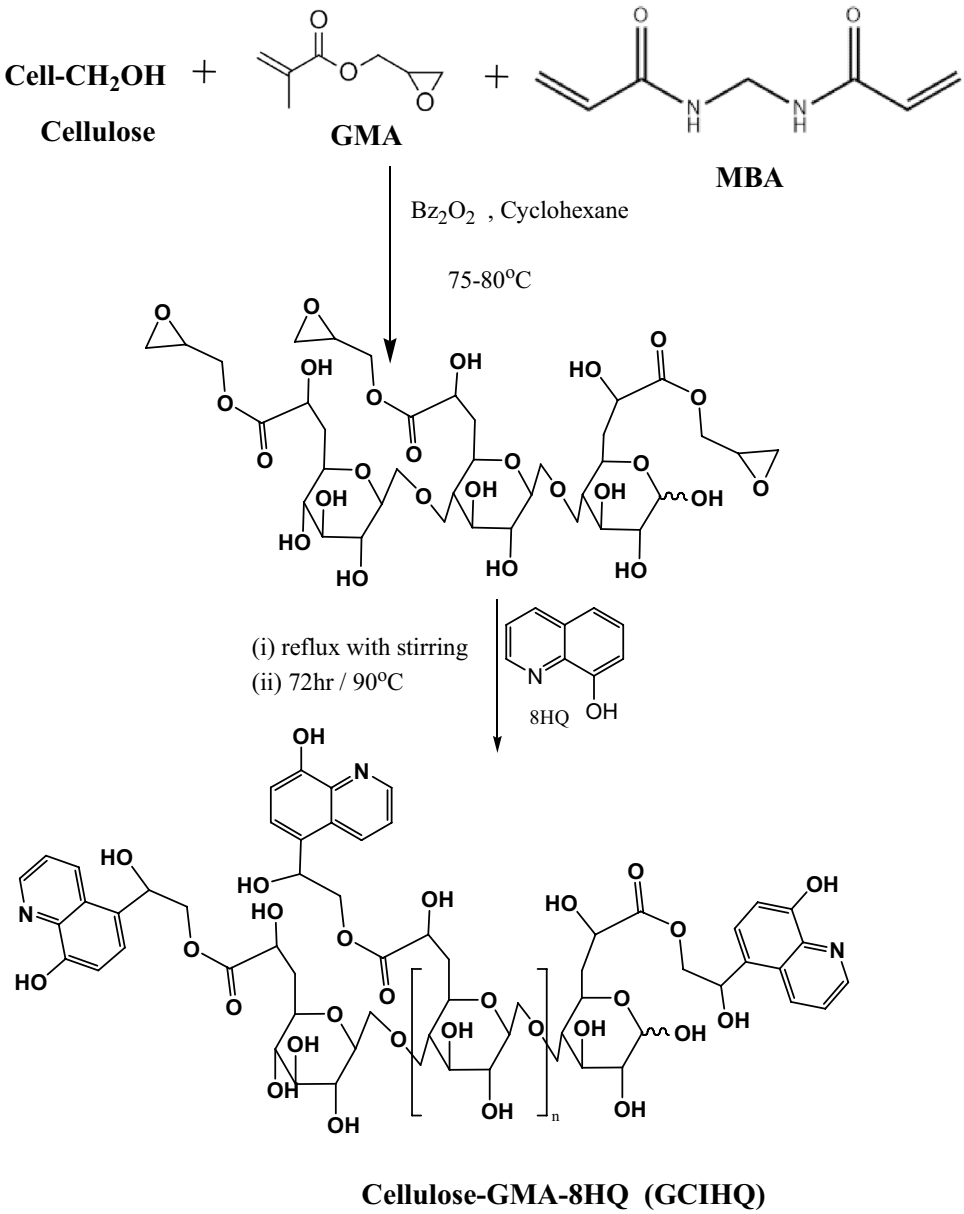

906 cm^{-1}, indicating that it is reacting with 8-hydroxyquinoline and also displayed new bands at 1457 and 1385 cm^{-1} referred to the presence of oxine group cm^{-1} [28, 40, 44]. These findings ensured the successful synthesis of GCIHQ. Furthermore, it was evident that the adsorption of V(V) ions among GCIHQ generally lead to decreasing in the intensity of FTIR peaks at 1723, 1457, 1163, 1112, 1058 cm^{-1}, as seen in Fig. 1a.

TGA Analysis

TGA measurements were also used to evaluate the performance of the cellulose modifications, as shown in Fig. 1b. The thermogram of cellulose showed thermal stability up to 300 °C followed by a sharp weight loss that was obtained in a temperature range of 300 to 360 °C. Between 360 and 500 °C, the cellulose started a gradual degradation stage. On the other side, for GCIHQ, a degradation stage has occurred with a weight loss of 8% in the temperature range of 21–155 °C, then thermal stability was attained up to 291 °C. From 219 and 500 °C, a gradual degradation stage with a weight loss of about 70% has happened, which

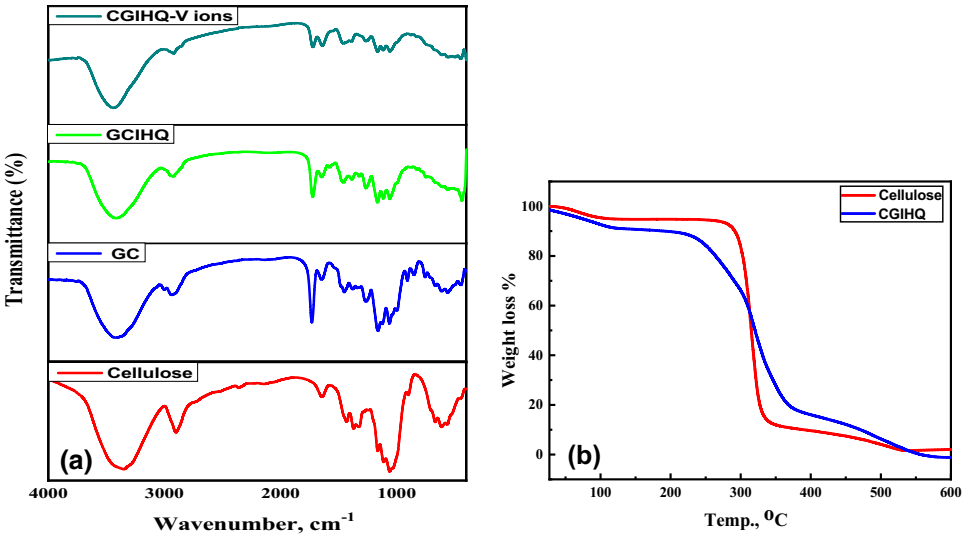

Fig. 1 IR-spectra of cellulose, GC, GCIHQ before and after V(V) ions adsorption (**a**); TGA of cellulose and GCIHQ (**b**)

indicated that the cellulose has slightly higher stability than GCIHQ.

Morphology and Textural Properties

SEM analysis was used to develop a surface micrograph of GCIHQ before and after adsorption of V(V) ions, as shown in Fig. 2a, b. It should be noticed that EDX spectrum is better to be measured for large surface area of the sample for better representation [41]. That means the SEM image from which EDX is measured could be in µm scale. The image of GCIHQ-V showed a large particle with a closely packed plane surface with a bright appearance, which could be related to coverage of GCIHQ's surface with vanadium ions. Also EDX measurements verified this. In Fig. 2b, the sorbent showed signals at 4.90 k.e.V, corresponding to the adsorbed V(V) ions on GCIHQ /V(V) ions if compared with the free GCIHQ sorbent. Surface area, pore volume, and average pore size were measured and reported to be 65.9 m^2/g, 22.5 cc/g, and 681.8 nm, respectively. These findings showed that GCIHQ has a higher surface area than that of cellulose itself (21.7 m^2/g) [45]. The isotherm of GCIHQ (Fig. 2d) showed a hysteresis loop characteristic. The isotherm can be categorised as an H1 type, which has a long extended cylindrical pore type [46]. No obvious change in weight or shape of GCIHQ sorbent after soaking for 24 h in alkali or acid media was detected, so this proved that the modified sorbent has good durability in both mediums.

Experimental Studies

pH Factor

The vanadium species in an aqueous solution have a direct effect on their behavior during the recovery processes. The polymeric degree of vanadium in an aqueous solution, which varies between 2 and 10, depends on its vanadium concentration and the solution`s acidity value [47]. Lower concentrations (less than 10–4 M) of vanadium ions exist as mononuclear species in the + 4 and + 5 oxidation states throughout the pH range. To examine the chemical forms of vanadium species in solutions, a simulation has been performed using MEDUSA software and distribution of V(V) species as a function of pH (Fig. 3a, b) [48]. The impacts of pH value on V(V) ions adsorption on GCIHQ sorbent through batch mode tests with fixed conditions of 20 mg sorbent, 2 h, and 20 ml aqueous solution assaying 200 mg/L V(V) ions were conducted in a range of 1.0 to 5.0 at ambient temperature (Fig. 3c). As can be seen from Fig. 3c, the adsorption efficiency of V(V) ions increased with increasing the pH from 1.0 to 4.0 then decreased by enhancing the pH over 4.0. At pHs below 4.0, low uptake efficiencies were detected that might be due to the competition of the protons present in the medium and vanadium ions towards the active groups of the sorbent. Furthermore, the diminishing in the adsorption uptake, at pH higher than 4.0, might be due to electrostatic repulsion between V anionic species (which appeared in this pH region as shown in Fig. 3a, b) and the negatively charged surface of the adsorbent. The presence of V(V) ions in the form of positive species coordinated with the hydroxyl and secondary amine groups (donor atoms, Fig. 3d) may explain the highest uptake value of 113 mg/g at pH 4.0. According to the findings, the pH value is a critical element in achieving high vanadium ion adsorption potential from aqueous phases. The proposed mechanism of the interaction between the V(V) ions and the active sites on the synthesized GCIHQ sorbent can be shown in Fig. 3d.

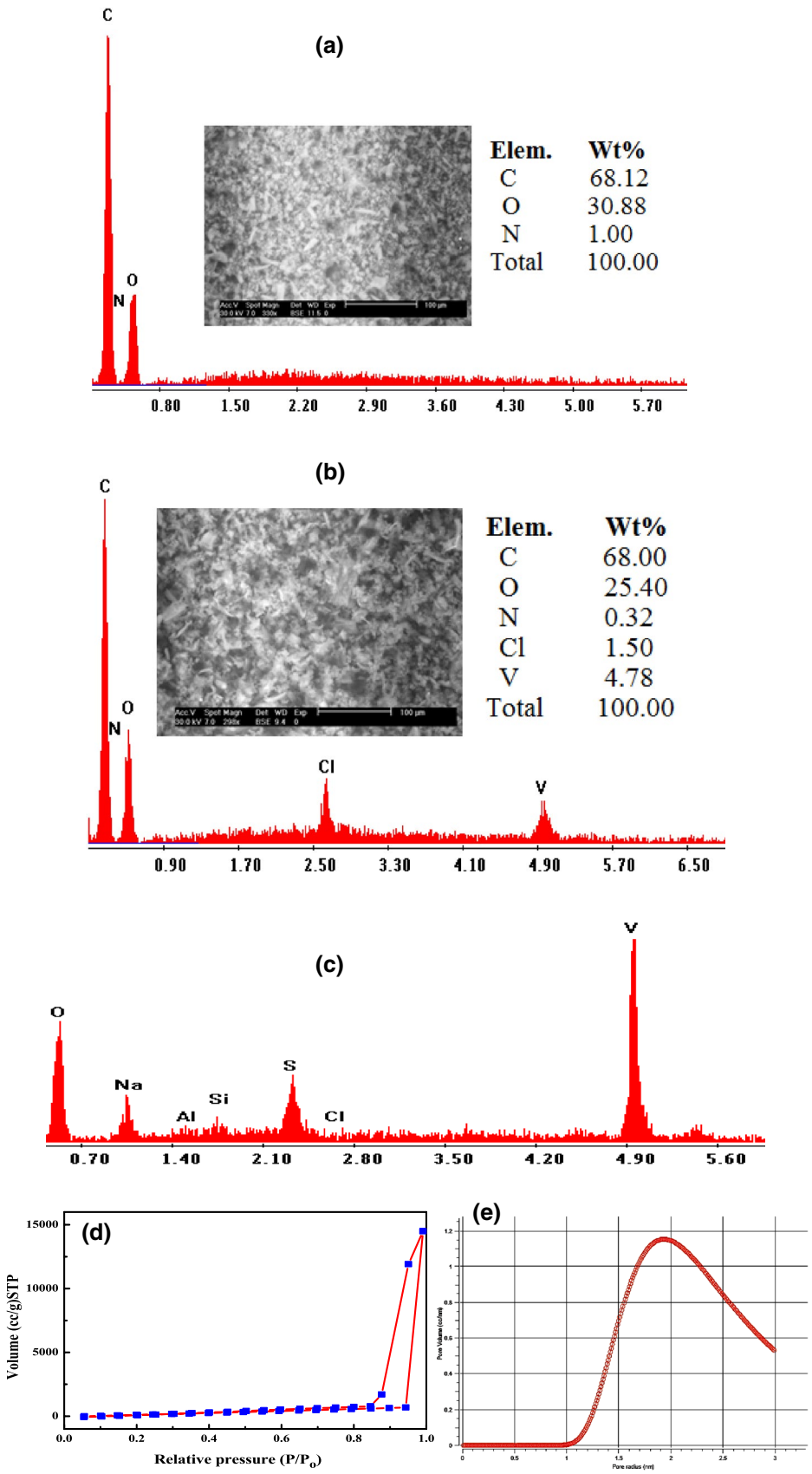

Fig. 2 SEM–EDX analysis for GCIHQ before adsorption of V(V) ions (**a**); after adsorption (**b**); EDX-chart for final product produced from treatment of a real sample (**c**); Nitrogen adsorption/desorption isotherms for GCIHQ sorbent (**d**, **e**)

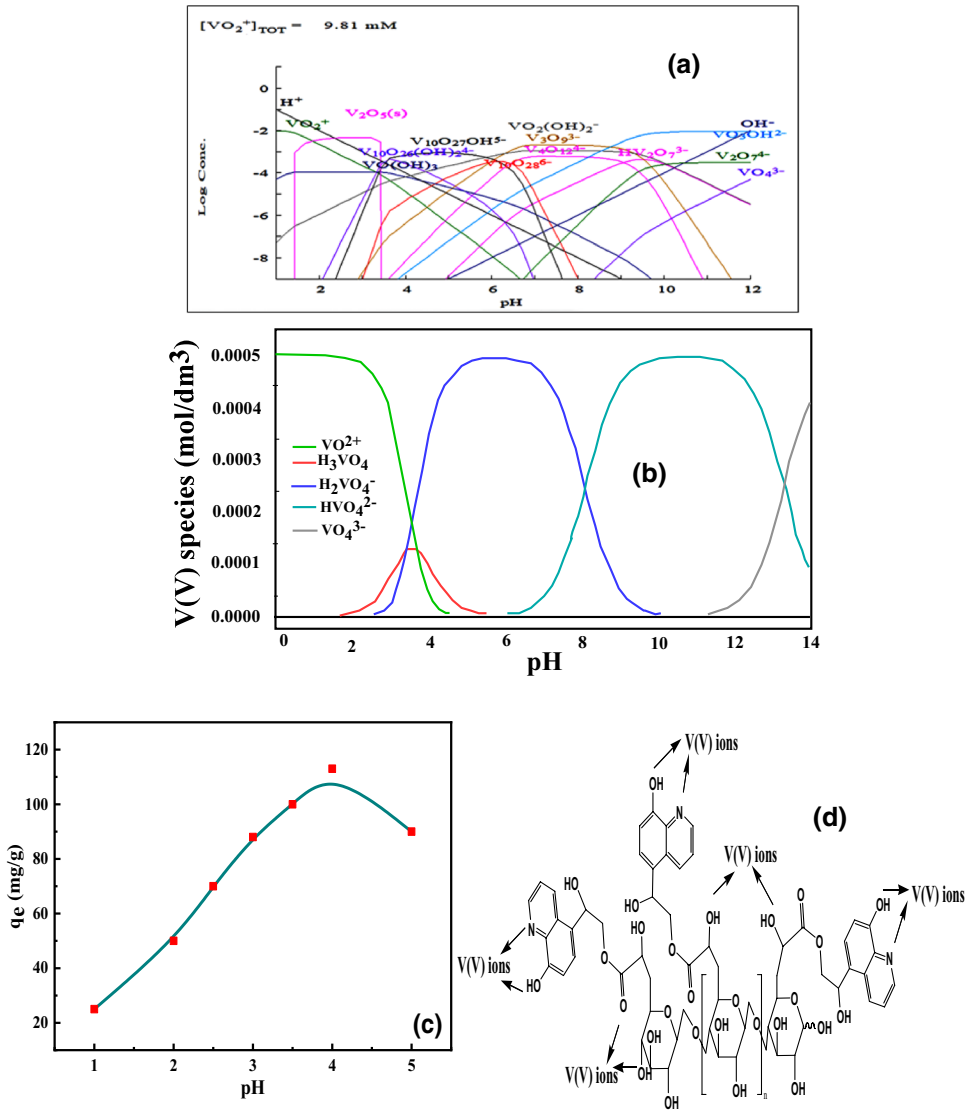

Fig. 3 Expected species of vanadium ions and its distribution at different pHs (**a**, **b**); Effect of pH on the adsorption of V(V) ions on GCIHQ (**c**); Proposed mechanism of interaction of V(V) ions with GCIHQ (**d**)

Contact Time Factor and Kinetic Investigations

The uptake of V(V) ions as a time—dependent must be observed in order to study the kinetics of the process. 10 mL aqueous solution fractions of 200 mg/L starting vanadium concentration at pH 4.0 were agitated separately for 15 to 120 min at room temperature with 10 mg GCIHQ sorbent. As shown in Fig. 4a, although roughly half of total adsorption was obtained in the first 30 min, the full adsorption uptake was reached in 60 min. The high concentration of V(V) ions and the availability of active sites on the GCIHQ sorbent were attributed to the high adsorption efficiency.

The adsorption data in Fig. 4a were investigated using PFO, PSO, and intra-particle diffusion theories to verify the kinetics of the adsorption reaction. Calculating the correlation coefficient values of straight lines (R^2) as well as comparing the experimental and calculated values of q_e were used to verify the models' validity. The PSO kinetics model had a higher R^2 than the PFO kinetics model (Fig. 4c and Table 3). Furthermore, the PSO model reported theoretical adsorption uptake of V(V) ions on GCIHQ was closer to the actual value than the PFO model. The PSO model suggests that the interaction between the adsorbent and the adsorbate is achieved through a chemical process, hence the adsorption of V(V) ions on the produced GCIHQ was chemical [49]. The uptake versus time results for adsorption were evaluated according to the Fickian diffusion relation to explore intra-particle diffusion and the rate of adsorption. As shown in Fig. 4d, Plotting qt vs $t^{0.5}$ gave a straight line passing through the origin. It was an indication that intraparticle ion diffusion through the pores impacted the rate of adsorption [50].

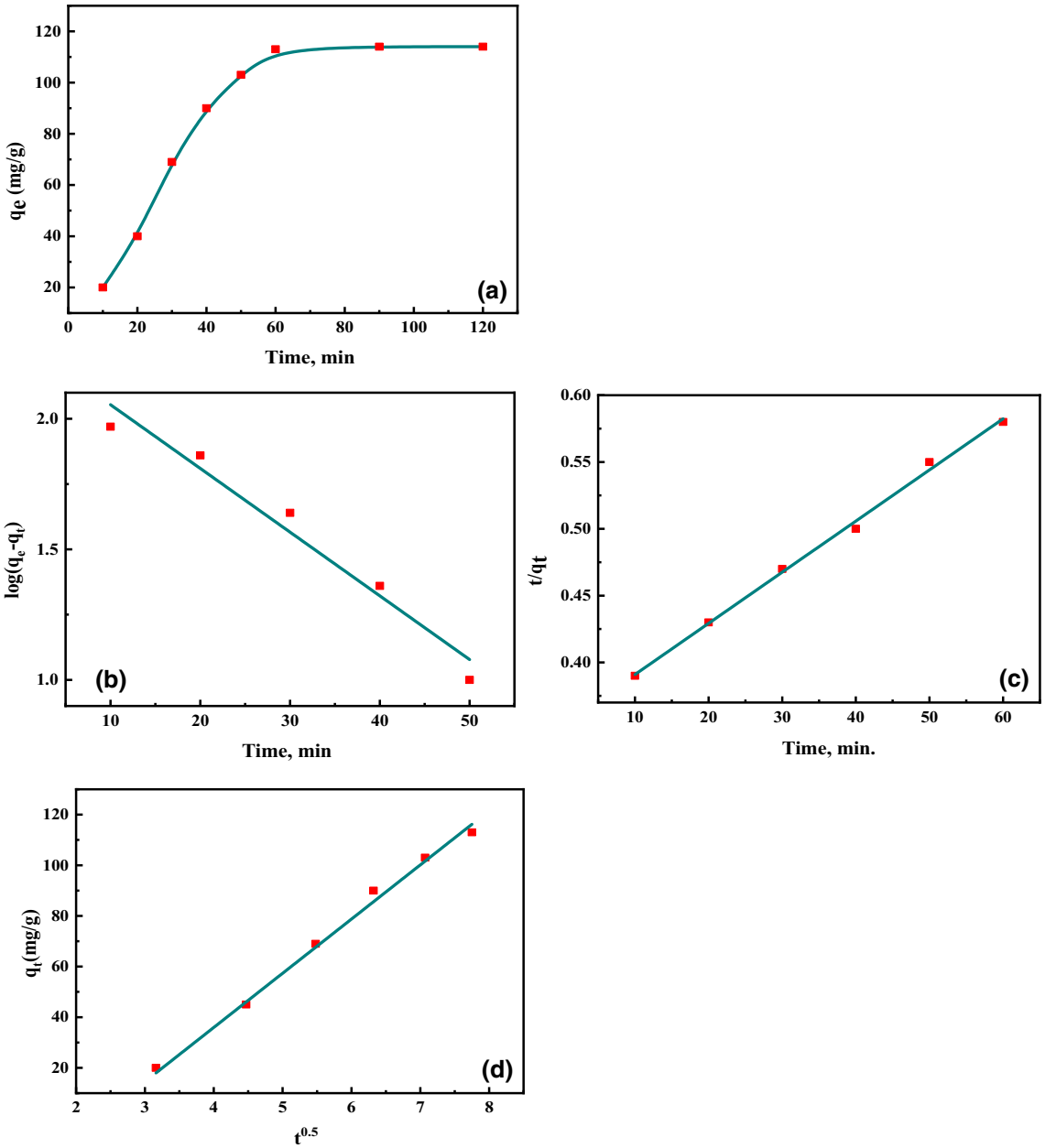

Fig. 4 Effect of contact time on the adsorption of V(V) ions on GCIHQ (**a**); PFO plot for the adsorption process (**b**); PSO plot for the adsorption process (**c**); Intraparticle diffusion plot for the adsorption process (**d**)

Table 3 Kinetic parameters for the adsorption of V(V) ions on GCIHQ

Temp, K	q_e exp	PFO model			PSO model			Intra-particle diffusion		
	mg/g	K_1, min^{-1}	q_e calc mg/g	R^2	K_2, min^{-1}	q_e calc mg/g	R^2	K_i, min^{-1}	X	R^2
298	113.00	0.0560	199.00	0.951	0.0001	120.00	0.996	21.39	−49.60	0.986

Sorbent Dose Factor

The target of this factor was to explore GCIHQ impact on the adsorption of V(V) ions. For 60 min at 25 °C, 20 mL of a solution containing 200 mg/L of V(V) ions at pH 4.0 was mixed with different quantities of GCIHQ ranging from 10 to 50 mg. Increasing the amount of GCIHQ sorbent increased the uptake of V(V) ions, as seen in Fig. 5a. This

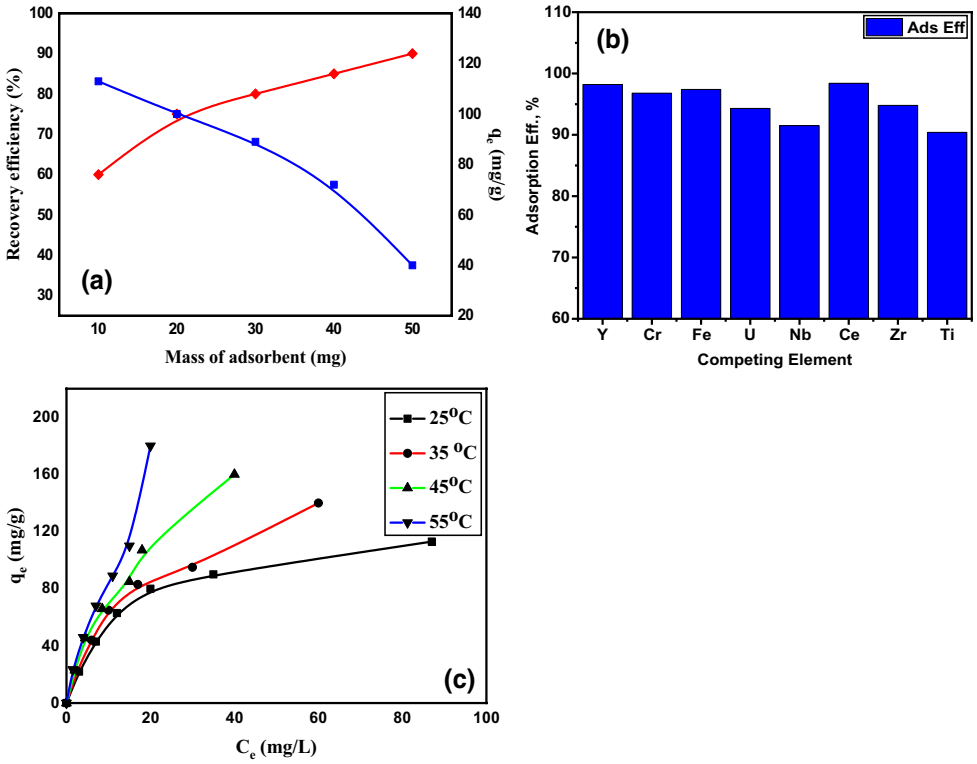

Fig. 5 Effect of sorbent dose on the adsorption of V(V) ions on GCIHQ (**a**); Effect of co-existing ions on the adsorption of V(V) ions on GCIHQ (**b**); Effect of initial concentration on the adsorption of V(V) ions on GCIHQ at different temperature (**c**)

could be explained by the increased sorbent dose causing a greater availability of active sites. However, no considerable improvement was observed in the extraction efficiency with a further increase in the sorbent dose from 113 mg/g. This suggested that after a certain dose of sorbent, surface area decreased as a result of the agglomeration of the sorbent, so the number of free ions available for further adsorption decreased [51].

Co-Existing Ions Factor

The effects of common ions in waste solutions such as Y, Cr, Fe, U, Nb, Ce, Zr, and Ti were studied. The concentration of the co-existing ions and the initial V(V) ions concentration of 200 mg/L concentrations were prepared under the optimized adsorption conditions. As seen in Fig. 5b, there was no obvious effect from the presence of the other ions on V(V) ions adsorption efficiency. In all of this set of trials, the adsorption efficiencies exceeded 90%, showing that the sorbent function group can retrieve V(V) ions from real effluent solutions effectively.

Initial V(V) Ions Concentration and Adsorption Temperature Factor

The initial concentration serves as the main driver in resolving all vanadium ions' mass transfer resistance between the liquid/solid phases. The effect of the initial V(IV) ions concentration on the adsorption efficiency on sorbent was studied in the range from 25 to 200 mg/L under fixed conditions at four different temperatures: 25, 35, 45, and 55 °C. At various V(V) ions concentrations, different qe values were calculated; the larger the initial vanadium ions concentration C_i, the greater the number of V(V) ions bonded to the GCIHQ sorbent at equilibrium (Fig. 5c). This could be explained by increasing the competition between the vanadium ions found in a large concentration with the same active site. As a result, the maximum adsorption capacity of V(V) ions on GCIHQ sorbent was reported to be 113 mg/g. at ambient temperature and increased to 180 mg/g with increasing temperature to 55 °C. Comparing to other sorbents (Table 4) [4, 52–58], GCIHQ exhibits higher uptake capacity and affinity towards V(V) ions; on the other hand, its chemical stability and ease of synthesis suggested that it may be a convenient sorbent in vanadium recovery technology.

Adsorption Isotherms

Isotherm is the relationship between the concentrations of a solid and fluid, used to describe states of no change in the sorption process. To depict the mechanics of the process, several isotherm models were examined. A proper understanding and interpretation of adsorption isotherms are critical for the overall improvement of adsorption mechanism pathways and the effective design of the adsorption systems

Table 4 Comparison of loading capacities of synthesized GCIHQ and other sorbents for vanadium ions

Adsorbent	Capacity (mg/g)	Ref
Multi-walled carbon nanotubes	375.94	52
Chitosan–silica composite	244.51	53
Magnetized natural zeolite polypyrrole	65.00	54
Bisphosphonate nano-cellulose	100.86	4
Zr(IV)-loaded orange juice residue	51.09	55
Fe activated carbon	119.01	56
Anion exchange (Amberjet TM 4200 Cl)	48.90	57
Commercial-activated carbon	37.87	56
Starch waste sludge	37.17	58
Shale and Coal waste	75.19, 59.88	13
Leucine modified cellulose	54.00	5
GCIHQ sorbent	113.00	This study

[59]. Langmuir and D-R isotherms assume that adsorption occurs in a monolayer with no competition for adsorption between the adsorbed sites [60–62]. While Freundlich and Temkin's isotherms were used to test the multilayer formation of vanadium on GCIHQ sorbent.

Langmuir Model Graphing C_e/q_e vs. C_e with a slope equivalent to $1/Q_{max}$ and intercept equivalent to $1/K_LQ_{max}$ using the Langmuir adsorption model (Eq. 4) yielded a straight line (Fig. 6). The slopes and intercepts were used to calculate Q_{max} and K_L values for adsorption of V(V) ions at variable temperatures (Table 5). From the data in Table 5, it was noticeable that the Q_{max} values obtained from Langmuir plots for V(V) ions at all investigated temperatures were largely compatible with the experimental ones. The degree of suitability of GCIHQ towards vanadium ions was predicted by the Langmuir dimensionless separation factor (R_L) values. The separation factor, R_L, is given by Eq. 12. The results of the Langmuir isotherm constants were given in Table 5.

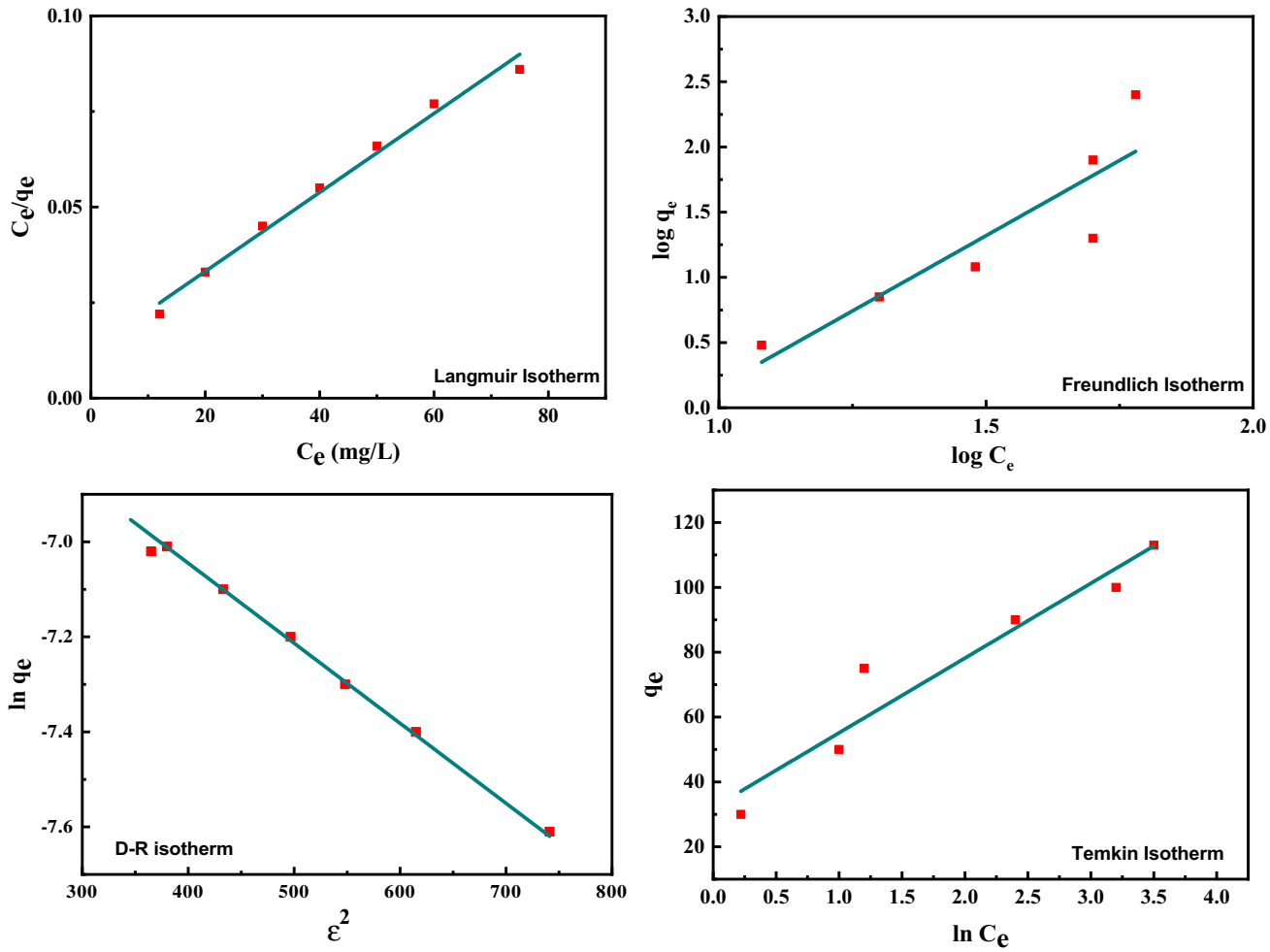

Fig.6 Adsorption isotherms curves for adsorption of V(V) ions on GCIHQ sorbent

Table 5 Adsorption isotherm parameters for adsorption of V(V) ions on GCIHQ sorbent

Temp.,°C	q_e, mg/g	Langmuir			Freundlich			D-R			Temkin		
		$Q_{max,}$ mg/g	$K_{L,}$ L/mg	R^2	K_f mg/g	n	R^2	K_{DR} mmol/g	B j^2/mol^2	E Kj/mol	b_T j/mol	A_T L/mol	R^2
25	113.00	125.00	0.008	0.986	0.007	0.4000	0.754	1.65	0.003	12.91	19.3	4.02	0.911

$$R_L = \frac{1}{1 + K_L C_o} \tag{12}$$

K_L: the Langmuir equilibrium constant, C_o: the initial concentration of the investigated metal ion. The adsorption process was determined to be irreversible ($R_L = 0$), favourable ($0 < R_L < 1$), and unfavourable ($R_L = 1$). The values of R_L for all concentration ranges were between 0.53 and 0.23 at ambient temperature, indicating that the adsorption technique was suitable.

Freundlich Model Graphing log q_e vs. log C_e (Fig. 6) yielded a straight line that was utilized to derive the Freundlich constant for the adsorption process of V(V) ions using the Freundlich adsorption model (Eq. 6). K_f and n values for V(V) ions were determined from the intercept and slope readings and are reported in Table 5.

D-R Isotherm The D-R isotherm's mean adsorption energy (E) (Eqs. 7–9) can provide useful information regarding these features. For E < 8 kJ/mol, physisorption being dominated the adsorption mechanism. If E is in the range 8–16 kJ/mol, the adsorption process follows the chemisorption mechanism. The B, E, and R^2 values (Fig. 6, Table 5) at ambient temperature were found to be 0.0.003 J^2/mol^2, 12.91 kJ/mol, and 0.996, respectively. The value of E suggested that V(V) ion adsorption on the sorbent is most likely due to a chemisorption mechanism. Increasing the temperature effective positively on the adsorption of V(V) ions on GCIHQ sorbent as the strength of bonding between the metal ion and resin clearly increased with the temperature.

Temkin Isotherm The adsorption heat of all molecules reduces linearly as the adsorbent surface is covered more, according to this isotherm model, and the adsorption process is defined by a uniform distribution of binding energies [63]. The isotherm includes a component that accounts for adsorbent–adsorbate interactions [64]. As illustrated in Fig. 6, several parameters (Eq. 10) were calculated by graphing q_e vs. lnC_e. The values of estimated Temkin parameters and the closest values of R^2 to 1 in Table 5 proved that the examined metal ions adsorbed chemically on the GCIHQ sorbent.

Adsorption conclusions from various isotherms were compared to describe the mechanism of the adsorption process in order to determine the best-fitting isotherm model. The adsorption capacity of the investigated adsorbent in the Langmuir isotherm for V(V) ions was so close to the GCIHQ adsorbent's realistic maximum saturation capacity, according to the findings. As a consequence, the adsorption process was largely monolayer and followed Langmuir and D-R isotherms at all temperatures, indicating that the Freundlich and Temkin models could not describe the adsorption of vanadium ions on GCIHQ.

Thermodynamic Calculations

Additionally, this study measured thermodynamic parameters such as Gibbs free energy (ΔG), enthalpy (ΔH), and entropy (ΔS). The values of K at different temperatures were processed according to van't Hoff Eqs. 13 and 14 to get the thermodynamic parameters of the adsorption reaction of V(V) ions on GCIHQ sorbent [37].

$$\ln K_L = \frac{-\Delta H}{R} + \frac{\Delta S}{RT} \tag{13}$$

$$\Delta G = \Delta H - T\Delta S \tag{14}$$

ΔH (kJ/mol) and ΔS (kJ.mol/K): enthalpies and entropy changes, respectively, R: the gas constant.

The straight lines with slope and intercept equal to ΔH/R and ΔS/R, respectively, were obtained by graphing ln K_L vs. 1/T, as shown in Fig. 7, where values of ΔH and ΔS were determined and presented in Table 6. The found positive values of ΔH for adsorption of V(V) ions on GCIHQ suggested that the adsorption process was endothermic, with the adsorption capacity increasing as the temperature increased. The values of ΔG were obtained and reported in Table 6. The negative values of ΔG obtained indicated that the adsorption process was feasible and spontaneous. The positive ΔS parameter suggested increasing the system randomness at the solid–liquid interface during the adsorption process. The fact that ΔG values decreased as temperature ascended suggested that the adsorption process was more conducive at higher temperatures. Data given in Table 5 showed a change in the value of $T\Delta S$ at all temperatures and $|\Delta H| < |T\Delta S|$. This indicated that entropic variations dominated the adsorption [65, 66]. When the standard deviation (SD) of the obtained

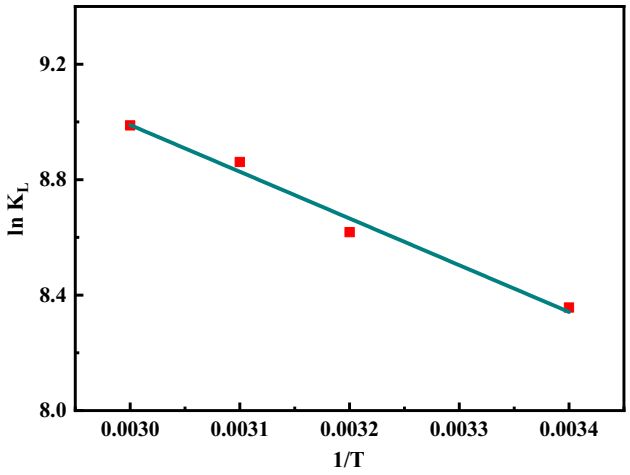

Fig. 7 Van't Hoff plot for adsorption of V(V) ions on GCIHQ sorbent

Table 6 Thermodynamic parameters for adsorption of V(V) ions on GCIHQ sorbent

ΔH KJ.mol^{-1}	ΔS J.mol^{-1}. K^{-1}	ΔG KJ.mol^{-1}			
		298 K	308 K	318 K	328 K
13.46	115.15	−34.30	−35.45	−36.60	−37.76

results was examined, it was obvious that the SD ranged between ± 0.3 and ± 0.5.

Desorption and Regeneration

The reusability and reuse of sorbents are critical to the effort estimation when commercial implementation is being considered. Desorption experiments were performed by using HCl and H_2SO_4 as desorption agents. Desorption efficiency of GCIHQ reached 98% for V(V) ions using 1 M H_2SO_4 beside achieved 93% for 1 M HCl as eluent. This conclusion pointed to the GCIHQ sorbent's excellent durability (with a standard variation of 0.1%) after five cycles with 1 M H_2SO_4, as the acquired data indicated that uptake capacity could be maintained above 95% after the third cycle.

Application on Non-Synthetic Sample

V(V) ions were recovered from waste solution supplied from NMA laboratories using manufactured GCIHQ adsorbent. The optimal regulatory parameters impacting the adsorption of the examined metal ions were chosen to treat this waste solution utilizing GCIHQ. The product produced after desorption of GCIHQ sorbent loaded with V(V) ions and increasing the pH of the solution to pH 7.5 was found to be effective in recovering V(V) ions from waste effluents, with a 90% recovery efficiency for V(V) ions with a small amount of interfering components as shown in the EDX chart of the product produced after desorption of GCIHQ sorbent loaded with V(V) ions and increasing the pH of the (Fig. 2c).

Conclusion

Durable, and stable GCIHQ sorbent using an inexpensive method was synthesized to be used as a sorbent for V(V) ions retrieval. pH, sorbent concentration, contact time, and starting V(V) concentration have impacted the uptake of V(V) ions on GCIHQ. GCIHQ sorbent was succeeded in V(V) ions adsorption from chloride solution with the uptake capacity of 113 and 180 mg/g under adsorption temperatures of 25 and 55 °C respectively at optimum solution pH 4. SEX-EDX and FT-IR analyses of the loaded sorbent proved the vanadium adsorption upon the GCIHQ sorbent. The equilibrium adsorption results were studied using various isotherms models which clarified the sorption process and provided insight into the mechanism of sorption. The adsorption reaction was discovered to follow PSO kinetics, and the estimated adsorbate in the adsorbent at equilibrium matched the experimental results quite well (R^2 of 0.99). Calculated activation energy (E_a) for adsorption (12.91 kJ. mol^{-1}) proved chemisorption process. The change in standard free energy (ΔG), enthalpy (ΔH), and entropy (ΔS) was calculated using thermodynamic equilibrium coefficients to determine that the reaction was endothermic in nature and that the adsorption process was more favored at higher temperatures. By the optimization of parameters, the desorption percentages of V(V) ions were found to be 98% using 1 M H_2SO_4.

Acknowledgements The authors wish to thank the colleagues at Nuclear Materials Authority, Egypt, for their kindly following-up, scientific support, and great assistance in finishing this work.

Funding Open access funding provided by The Science, Technology & Innovation Funding Authority (STDF) in cooperation with The Egyptian Knowledge Bank (EKB). The authors have not disclosed any funding.

Declarations

Conflict of interest The authors declared no potential conflict of interest with respect to the research, authorship, and/or publication of this article. The authors have no relevant financial or non-financial interests to disclose. The authors declare that no funds, grants, or other support were received during the preparation of this manuscript.

References

1. Moskalyk RR, Alfantazi AM (2003) Min Eng 16:793–805
2. Marks S (1929) A textbook of inorganic chemistry Vol. VI. Part III. Charles Griffin & Company Limited, London
3. Erdem A, Shahwan T, Cagir A, Eroglu AE (2011) Chem Eng J 174:76–85
4. Sirvio JA, Hasa T, Leiviska T, Liimatainen H (2016) Cellulose 23(1):689–697
5. Yousif A, El-Afandy A, Dabbour G, Mubark AE (2020) J Disper Sci Technol. https://doi.org/10.1080/01932691.2020.1844018
6. Chandler H (1998) Metallurgy for the Non-metallurgist. ASM International, USA
7. Vanadium Data Sheet, Allegheny Technologies, Wah Chang. www.atimetals.com/documents/vanadium_v1.com Accessed 16 Jan 2009
8. Khorfan S, Wahoud A, Reda Y (2001) Chem Eng 45:131–137
9. L Perron (2001) The vanadium industry: a review. In: Tanner, M.F., Riveros, P.A., Dutrizac, J.E., Gattrell, M., Perron, L. (Eds.), Vanadium, Geology, Processing and Applications, Proceedings of the International Symposium on Vanadium, Conference of Metallurgists, Montreal, Canada, August 11, 17–27
10. Cappuyns V, Swennen R (2014) Environ Sci Pollution Res 21(3):2272–2282
11. Abbas A, Conway BE (2002) J Colloid Interf Sci 251:248–255
12. Namasivayam C, Sangeetha D (2006) Adsorption 12:103–117
13. Saleh TA (2021) Environ. Technol. Innovation 24:101821
14. Saleh TA (2020) Environ. Technol. Innovation 20:101067
15. Saleh TA (2020) Trends Environ Anal Chem. https://doi.org/10.1016/j.teac.2020.e00080
16. Kajjumba GW, Aydın S, Gu¨neysu S (2018) Adsorption. Sci Technol 36(3–4):936–952
17. Nwosu-Obieogu K, Dzarma G, Okolo B, Akatobi K, Aguele F (2021) Kem Ind 70(3–4):129–135
18. Li H, Zhang H, Dong MLY, Xu H, Cheng X, Caie Z (2021) Water Pract Technol 16(4):1410–1420
19. Hashad AH, Atiti SY, Cheira MF, Ghonaim AK (2011) Arab J Nucl Sci Appl 44(3):27–42
20. Cheira MF (2020) Chem Pap 74:2247–2266
21. Sivan SK, Padinjareveetil AKK, Padil VVT, Pilankatta R, George B, Senan C, Černík M, Varma R (2019) Clean Technol Environ Policy 21(8):1549–1561
22. Zhang P, Hou D, O'Connor D, Li X, Pehkonen S, Varma RS, Wang X, Sus ACS (2018) Chem Eng 6(7):9229–9236
23. Nasrollahzadeh M, Sajjadi M, Iravani S, Varma RS (2021) Carbohydr Polym 251:116986
24. OA Bin-Dahman, TA Saleh (2022) Biomass Conv Bioref. https://doi.org/10.1007/s13399-022-02382-8
25. Saleh TA, Mustaqeem M (2022) M Khaled 17:100617
26. TA Saleh, A Sarı, M Tuzen (2002) Biomass Conv Bioref. https://doi.org/10.1007/s13399-021-02163-9
27. Gan C, Liu M, Lu J, Yang J (2020) Water Air Soil Pollution 231:10
28. Xu C, Nasrollahzadeh M, Sajjadi M, Maham M, Luque R, Puente-Santiago AR (2019) Ren Sus Ener Rev 112:195–252
29. Marczenko Z (1986) Separation and Spectrophotometric Determination of Elements. Ellis Harwood, Chichester
30. Yousif AM, El-Afandy AH, Abdel Wahab GM, Mubark AE, Ibrahim IA (2015) J Radioanal Nucl Chem 303:1821–1833
31. Yousif AM, Labib SA (2016) J Disper Sci Technol 37:4
32. Dacrory S, Haggag EA, Abdo SM, Masoud AM, Eliwa AA, Kamel S (2020) Cellulose 27:7093–7108
33. Hamza MF, Mubark AE, Wei Y, Vincent T, Guibal E (2020) Gels 6(2):12
34. AA Eliwa, AE Mubark (2021) Inter J Environ Anal Chem. https://doi.org/10.1080/03067319.2021.1921762
35. Langmuir I (1918) J Am Chem Soc 40:1361
36. Freundlich H (1906) Phys Chem Soc 40:1361
37. Foo KY, Hameed BH (2010) Chem Eng J. https://doi.org/10.1016/j.cej.2009.09.013
38. Tempkin MI, Pyzhev V (1940) Acta Phys Chim USSR 12:327–356
39. Marinich JA, Ferrero C, Jimenez-Castellanos MR (2009) Eur J Pharm Biopharm 72:138–147
40. Zhao Y, Huang M, Wu W, Jin W (2009) Desalination 249:1006–1011
41. Saleh TA (2015) Environ Sci Poll Res 22(21):16721–16731
42. Saleh TA, Gupta VK (2012) Curr Nanosci 8:739–743
43. Saleh TA (2017) J Clean Prod 172:2123–2132
44. Saleh TA (2011) Appl Surf Sci 257:7746–7751
45. Silverstein RM, Baddler GC, Morrill TC (1991) Spectrometric identification of organic compounds, 5th edn. Wiley, Hoboken
46. Vishwakarma RK, Shivhare US, Nanda SK (2013) Food Bioprocess Technol 6:1355–1364
47. Zhang J, Zhang W, Zhang L, Gu S (2014) Solvent Extr Ion Exch 32:221–248
48. Suru˘ci´c L, Tadi´c T, Janji´c G, Markovi´c, B, Nastasovi´c A, Onjia A (2021) Metals 11:1777
49. Kapnisti M, Noli F, Misaelides P, Vourliasc G, Karfaridisc D, Hatzidimitrioua A (2018) Chem Eng J 342:184–195
50. Mubark AE, Hakem HA, Zaki EG, Elsaeed SM, Abdel-Rahman AA-H (2022) Inter. J Environ Sci Technol. https://doi.org/10.1007/s13762-021-03857-3
51. Peacock CL, Sherman DM (2004) Geochim Cosmochim Acta 68:1723–1733
52. Yu Y, Wei Q, Li J, Yang J (2017) Fuller Nanotub Carbon Nanostructures 25(3):170–178
53. Budnyak TM, Tertykh VA, Yanovska ES, Kołodyńska D, Bartyzel A (2015) Adsorpt Sci Technol 33(6–8):645–657
54. Mthombeni NH, Mbakop S, Ochieng A, Onyango MS (2016) J Taiwan Institute Chem Eng 66:172–180
55. Sharififard H, Soleimani M (2015) R Soc Chem 5:80650–80660
56. Hu Q, Zhao J, Huo F, Inoue K, Liu H (2014) Chem Eng J 248:79–88
57. Kera¨nen A, Leiviskä T, Salakka A, Tanskanen J (2015) Desalin Water Treat 53(10):2645–2654
58. Dog˘an V, Aydın S (2014) Sep Sci Technol 49(9):1407–1415
59. Ayawei N, Ebelegi AN, Wankasi D (2017) J Chem. https://doi.org/10.1155/2017/3039817
60. El-Khaiary MI (2008) J Hazar Mater 158(1):73–87
61. Abd El-Magied MO, Tolba AA, El-Gendy HS, Zaki SA, Atia AA (2017) Hydrometallurgy 169:89–98
62. Alharthi S, Abd El-Magied MO (2021) Korean J Chem Eng 38(11):2365–2374
63. Piccin JS, Dotto GL, Pinto LAA (2011) Braz J Chem Eng 28:295–304
64. Dada AO, Olalekan AP, Olatunya AM, Dada O (2012) J Appl Chem 3:38–45

65. Gujar RB, Mohapatra PK (2015) RSC Adv 5:24705–24711
66. A Alharbi, AA Gouda, BM Atia, MA Gado, AA Alluhaybi, J Alkabli (2022) Rus J Inorg Chem 67:560